Magnetic Tweezers-Based Force Clamp Reveals Mechanically Distinct apCAM Domain Interactions

Devrim Kilinc,[†‡] Agata Blasiak,[†§] James J. O'Mahony,[†] Daniel M. Suter,[¶] and Gil U. Lee[†‡*]
[†]School of Chemistry and Chemical Biology and [‡]Conway Institute for Biomolecular and Biomedical Research, University College Dublin, Belfield, Dublin, Ireland; [§]Institute of Biotechnology, Faculty of Chemistry, Warsaw University of Technology, Warsaw, Poland; and [¶]Department of Biological Sciences, Purdue University, West Lafayette, Indiana

ABSTRACT Cell adhesion molecules of the immunoglobulin superfamily (IgCAMs) play a crucial role in cell-cell interactions during nervous system development and function. The *Aplysia* CAM (apCAM), an invertebrate IgCAM, shares structural and functional similarities with vertebrate NCAM and therefore has been considered as the *Aplysia* homolog of NCAM. Despite these similarities, the binding properties of apCAM have not been investigated thus far. Using magnetic tweezers, we applied physiologically relevant, constant forces to apCAM-coated magnetic particles interacting with apCAM-coated model surfaces and characterized the kinetics of bond rupture. The average bond lifetime decreased with increasing external force, as predicted by theoretical considerations. Mathematical simulations suggest that the apCAM homophilic interaction is mediated by two distinct bonds, one involving all five immunoglobulin (Ig)-like domains in an antiparallel alignment and the other involving only two Ig domains. In summary, this study provides biophysical evidence that apCAM undergoes homophilic interactions, and that magnetic tweezers-based, force-clamp measurements provide a rapid and reliable method for characterizing relatively weak CAM interactions.

INTRODUCTION

There is growing interest in cellular mechanotransduction thanks to recent advances in experimental techniques that facilitate force application to cells and novel cell-culture systems with controlled mechanical properties and shapes (1). Force-induced changes in conformation, post-translational modification, and assembly of proteins have long been considered to act as switches that modulate intracellular signaling pathways (2). However, the dynamic nature of subcellular structures, such as focal adhesions, suggests that mechanotransduction mechanisms that are more dynamic than simple protein switches are required. These dynamic mechanisms should be able to sense variations in the rate, frequency, and duration of applied forces and respond accordingly (3). Therefore, it is becoming increasingly important to distinguish the various types of intra- and intermolecular bonds employed by mechanosensitive proteins and protein-protein complexes in order to understand dynamic phenomena such as cell adhesion and cell motility.

Cell-cell adhesion is based on noncovalent interactions between membrane-bound cell adhesion molecules (CAMs), many of which contain tandem repeats of structural motifs in a multimodular fashion (4). This multimodular structure is also common to extracellular matrix proteins such as fibronectin (Fn), and to intracellular proteins involved in mechanotransduction, such as talin (4). CAMs of the immunoglobulin superfamily (IgCAMs) consist of glycoproteins that contain multiple Ig-like domains and fibronectin type III (Fn III)-like domains in their extracellular portion. IgCAMs mediate adhesion to other cells and to the extracellular matrix through homophilic or heterophilic *trans* interactions. They can also form *cis* interactions on the same cell surface, leading to zipper-like structures (5). Intracellular portions of IgCAMs are anchored to cytoskeletal proteins and are able to trigger or modulate a number of signaling processes in response to extracellular stimuli (6). The IgCAM known as neural CAM (NCAM) is particularly well studied because of its important role in nervous system development and function, especially in neurite outgrowth (7).

Although many studies have provided insight into NCAM binding and function in vertebrate neurons, little is known about the biophysical mechanisms of how NCAM mediates adhesion and outgrowth through regulation of the cytoskeleton. This is largely because it is challenging to perform a quantitative analysis of cytoskeletal dynamics and mechanical properties in vertebrate growth cones. Due to their large size, *Aplysia* neurons represent an attractive model system for studying growth cone motility and cytoskeletal reorganization (8–14). *Aplysia* CAM (apCAM) has been considered to be the homolog of vertebrate NCAM because both molecules consist of five Ig-like and two Fn III-like repeats; however, NCAM and apCAM share only 26% amino acid identity (15). apCAM is involved in neurite fasciculation (16), memory-related synapse formation (17), and long-term facilitation (18). Studies with apCAM-coated beads revealed that this CAM can functionally associate with the actin cytoskeleton in two major ways: 1), apCAM clustering triggers site-directed actin assembly (19); and 2), apCAM acts as a force transducer in adhesion-evoked growth through coupling to the underlying retrograde actin

Submitted February 4, 2012, and accepted for publication August 8, 2012.

*Correspondence: gil.lee@ucd.ie

Editor: Denis Wirtz.

0006-3495/12/09/1120/10 $2.00

http://dx.doi.org/10.1016/j.bpj.2012.08.025

flow (20). This mechanical coupling has an intermittent, stochastic character (21) and is regulated by Src family tyrosine kinase activity (22). Although the role of apCAM in growth cone mechanotransduction is well established, the binding properties of apCAM interactions have not been characterized.

The kinetic and energetic properties of protein-protein interactions can be analyzed through the application of an external force. The energy landscape of a chemical reaction may contain one or more sharp activation barriers that need to be overcome for the reaction to occur. External force application increases the unbinding rate by skewing this energy landscape (23–25). According to Bell's model, the off-rate of a single, specific intermolecular interaction depends on the externally applied constant force, F:

$$k_{off} = k_{off,0} \exp\left(\frac{F}{f}\right) \quad (1)$$

where $k_{off,0}$ is the dissociation rate of the interaction in the absence of an external force, and f is the scaling force characteristic of that interaction (24). This model implies that weak, noncovalent bonds have a limited lifetime and will break under any level of force if they are pulled on for a sufficient time period. An extension of this model has been proposed (26) for multiple parallel bonds of the same type, where the off-rate also depends on the number of bonds, n:

$$k_{off} = k_{off,0}\left(\sum_{i=1}^{n}\left(\exp\frac{(-F/(i \cdot f))}{i}\right)\right)^{-1} \quad (2)$$

Although the dynamic strength of a bond seems to be greatly affected by the rate rather than the magnitude of the applied force, the force acting on an individual cell adhesion bond may build up as slowly as 1 pN/s and can break at a few piconewtons (27). This calls for force-clamp experiments in which Bell's model can be explicitly applied to determine the mechanical parameters of inter- and intramolecular bonds.

The magnetic-tweezers technique is based on the noninvasive manipulation of magnetic particles via an externally imposed magnetic field gradient. In the simplest case, particles can be pulled away from the imaging plane on an inverted microscope toward a permanent magnet assembly (Fig. 1 *A*). The fraction of particles remaining on the surface can be traced over time and provides a measure of the average lifetime of the bond holding the particle on the substrate (28). The application of external force on a single-molecule bond is demonstrated in Fig. 1 *C*, where increasing external force decreases bond lifetime according to Eq. 1. A single-molecule bond involving two types of interactions can lead to a spectrum of bond lifetime responses, depending on the relative kinetic and mechanical strengths of the

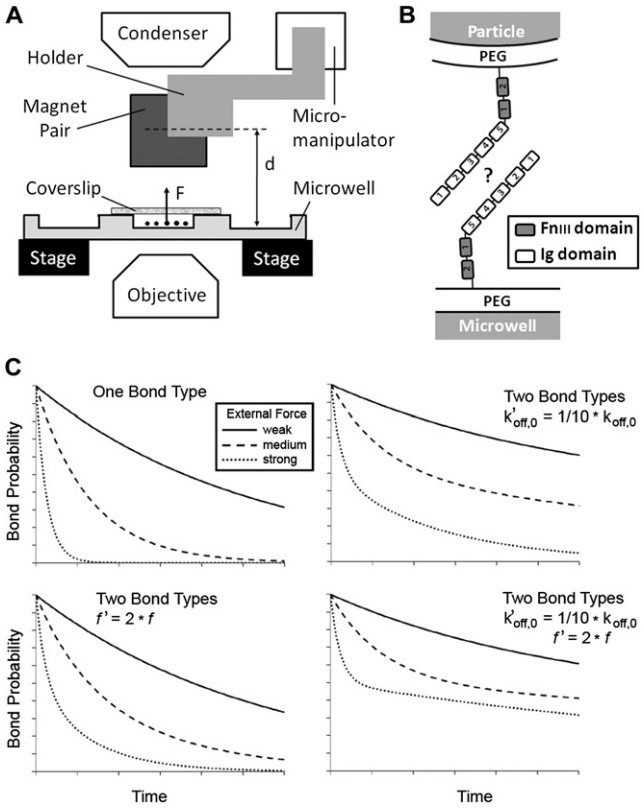

FIGURE 1 (*A*) Schematic of the experimental setup. Magnet pairs are positioned such that their same poles face each other with a gap of 1 mm, which enables imaging during magnetic force application. The imaging plane is the bottom of the microwell, where the superparamagnetic particles settle and apCAM homophilic interactions take place. (*B*) Schematic of apCAM homophilic interaction between particle and microwell surfaces. The extracellular portion of apCAM consists of two fibronectin type III domains and five Ig-like domains. (*C*) Simulation of the lifetime of a single-molecule bond for various hypothetical bond types based on Bell's model (24). Variation in the kinetic and mechanical strengths results in different force–bond lifetime curves for a single-molecule bond involving two types of interactions.

bond types present. This is particularly important in the case of IgCAMs, where the multimodular domain structure may be providing these molecules with the mechanical and subsequently functional flexibility that is required for their role in cellular mechanotransduction. Several lines of evidence suggest that homophilic NCAM adhesion is indeed mediated by multiple types of bonds (29–33), although the relative roles of individual Ig domain interactions have been a matter of debate (29,34,35). Characterization of the kinetic and mechanical properties of apCAM interactions therefore provides further insight into IgCAM-mediated cell adhesion mechanisms.

Although NCAM interactions have been characterized extensively with the use of biochemical (29), structural (34), and biophysical methods (32,35), no such information is available for apCAM, which has structural and functional similarities to NCAM. In this work, we used magnetic tweezers to measure the lifetime of homophilic apCAM bonds by

applying constant, physiologically relevant forces to the complete extracellular region of apCAM (Fig. 1 *B*). Mathematical modeling revealed that distinct bonds with similar mechanical kinetic properties mediate the homophilic apCAM interaction. The magnetic-tweezers technique offers relative ease in conducting and interpreting measurements, and thus enables rapid and potentially parallel screening of multiple molecular interactions.

MATERIALS AND METHODS

Magnetic-tweezers system and force calibration

Superparamagnetic microspheres (Ø = 1.25 μm; coefficient of variation (CV) $\leq$ 12%) were synthesized using an emulsion-based self-assembly technique that produces microparticles composed of uniform Fe_3O_4 nanospheres 90% by weight (36). The magnetic field was imposed by two pairs of NdFeB magnets (12.7×12.7×6.35 mm per pair) with their same poles facing each other over a 1 mm air gap (28). An aluminum magnet holder attached to a micromanipulator (Eppendorf, Hamburg, Germany) positioned the magnets over the imaging field of an inverted microscope (Zeiss, Hertfordshire, UK) at desired distances from the particles. A 20 μl particle suspension, containing 55,000 particles, was added to a polystyrene microwell (Nunc, Rochester, NY) and covered with a glass coverslip (Menzel, Braunschweig, Germany). Particles were imaged with phase contrast using a 40× objective. A schematic of the setup is shown in Fig. 1 *A*. Particle magnetic properties were measured on a superconducting quantum interference, device-based, magnetic properties measurement system (MPSP-SQUID; Quantum Design, San Diego, CA), in which Dynal MyOne beads (Invitrogen, Carlsbad, CA) were used as reference. The force acting on a magnetic particle was calculated from the drag velocity in a viscous fluid (see Supporting Material for details).

Conjugation chemistry

Self-assembling monolayers of polyethylene glycol (PEG) were used to minimize nonspecific adhesion between magnetic particles and the microwells, which can be on the order of nanonewtons (38). A mixture of methoxy- and amine-terminating PEGs were used to control the apCAM density on both surfaces. The ratio of amine-terminating PEG to total PEG was chosen to be 0%, 5%, or 20%. Particles were coated with polyethyleneimine (PEI; molecular mass (MM) = 1.3 kDa; Sigma, St. Louis, MO) via EDC/NHS (Pierce Biotechnology, Rockford, IL) chemistry. Polystyrene microwell surfaces were oxidized with trifluoroacetic acid (Sigma) before functionalization with PEI. Surfaces were then incubated with a defined mixture of methoxy-PEG-NHS (mPEG, MM = 2 kDa; Rapp Polymere, Tübingen, Germany) and BOC-protected amine-PEG-NHS (NH-PEG, MM = 3 kDa; Rapp) in high-salt carbonate buffer (0.6M K_2SO_4; pH = 8.2) at 50°C. Any residual free amine groups were capped by covalently linking them with β-mercaptoethanol (Sigma) after PEG incubation.

Recombinant His_6-tagged apCAM containing the extracellular portion was expressed by baculovirus-infected Sf9 cells and purified using nickel-nitrilotriacetic acid (Ni-NTA) agarose as previously described (39) (see Supporting Material for details). Two different methods were employed to conjugate apCAM protein to the protected amine groups on PEG-coated surfaces. In the so-called oriented method, amine groups on surfaces were first converted to carboxyl groups using methyl N-succinimidyl adipate (Pierce) and functionalized with N_α,N_α-Bis(carboxymethyl)-L-lysine hydrate (NTA; Sigma). NTA-coated surfaces were then reacted with apCAM (5 μg/ml in phosphate-buffered saline (PBS) containing 200 μM Ni^{2+}) overnight at 4°C. In the so-called nonoriented conjugation, primary amines of apCAM were converted to protected sulfhydryl groups using *N*-succinimidyl-S-acetylthioacetate (Pierce) at a molecular ratio of 1:4. Amine groups on surfaces were modified with sulfosuccinimidyl-4-(*N*-maleimidomethyl)cyclohexane-1-carboxylate (Pierce) and reacted with deprotected sulfhydryl groups on apCAM overnight at 4°C in PBS. The density of apCAM on PEG monolayers was measured via colorimetry (see Supporting Material for details).

Binding and forced unbinding assays

We conducted binding and unbinding assays by periodically imaging the microwell surface after introducing particles before and during magnetic force application. We quantified particle binding by analyzing the particle movement on microwell surfaces. Particles that were not bound to the surface exhibited a two-dimensional Brownian motion. We automatically extracted the particle trajectories using the tracking algorithm of AxioVision software (Zeiss). Particles were allowed to settle for 3 or 6 min on microwells before the magnetic force was applied. The time required to bring the magnet assembly over the microwell was $\leq$0.5 s. Particles were imaged at a high frame rate (4 fps) during the initial 30 s and a low frame rate (0.5 fps) during the following 240 s. The fraction of remaining particles was calculated by dividing the number of particles remaining on the surface to the number of bound particles before force application, as determined by their movement over the last 10–15 s of the settlement period.

Mathematical modeling and simulations

We developed a series of mathematical models to evaluate the data in a theoretical framework. The models consist of a series of equations that describe the association and dissociation kinetics of the bonds formed between particle and microwell surfaces. Individual Ig domain interactions within a single apCAM bond (Fig. 1 *B*) are modeled as point contacts that withstand the external force in a parallel fashion. These interactions fail one after another based on their k_{off} values and the external force is redistributed to the remaining ones. The particle leaves the surface when the last interaction fails. The models assume that 1), multiple bonds form in parallel (26); 2), the external force is equally distributed among the Ig domains involved; 3), bond formation occurs in a single step to form all Ig domain interactions simultaneously; and 4), no bond reformation occurs during external force application. Two conceptual models developed for the NCAM–NCAM interaction, model R and model L, are represented. Model R is based on the protein aggregation study by Ranheim et al. (29) and assumes engagement of all five Ig domains. Model L is based on force and molecular distance measurements obtained by the Leckband group (32,33,35) and enables two types of bonds, one involving five Ig domains (identical to model R) and the other involving only two Ig domains. Additional models were developed to include distinct states within Ig domain interactions that are modeled in series (Fig. S1). Binding and forced unbinding phases were simulated in tandem, and model parameters that produced the best fit to the experimental data were determined using an optimization scheme based on the random-walk method (40). The models, simulations, and curve-fitting algorithm are described in detail in the Supporting Material.

RESULTS

Characterization of magnetic particles and apCAM model surfaces

Our magnetic particles exhibit almost three times higher magnetic susceptibility than commercially available particles (Fig. S2 *A*). The force acting on a superparamagnetic microsphere is shown as a function of distance from the magnet assembly (Fig. S2 *B*). The magnetic force, but not the drag force, has a CV of 40% because it is proportional

to the volume of the particle. We estimated the apCAM coverage using a horseradish peroxidase (HRP)-based colorimetric assay, where the IgG density measured for the 0% apCAM constitutes the baseline. Fig. 2 *A* shows that apCAM surface density depends on both the conjugation chemistry and the fraction of NH-PEG employed. Estimating a PEG layer thickness of 5 nm (41) and an apCAM-apCAM doublet length of 31 nm (32), the contact area between a microsphere and a flat surface is calculated to be 0.127 μm^2. This corresponds to 4.1 $\pm$ 1.0 and 12.5 $\pm$ 4.1 oriented apCAM molecules (baseline density subtracted) per contact area for 5% and 20% NH-PEG ratios, respectively.

Oriented apCAM exhibits low nonspecific adhesion

We conjugated apCAM to the PEG layer using two different chemistries. Oriented conjugation incorporates the His_6-tag at the C-terminus of the protein, whereas nonoriented conjugation utilizes free amines on the protein. To determine the effect of molecular orientation on the apCAM bond, we conducted forced unbinding experiments varying the NH-PEG/mPEG ratio on either surface. Nonoriented apCAM exhibited a stronger interaction than oriented apCAM at the 20% NH-PEG ratio (Fig. S3). Of interest, nonoriented apCAM had much higher nonspecific adhesion compared with oriented apCAM in experiments in which only one surface had NH-PEG. We determined the level of nonspecific interactions for the oriented apCAM by examining the unbinding events under a higher force (Fig. 2 *B*). The level of nonspecific interaction in this model system was determined as <12.5% of particles remaining on the surface when 6.5 pN constant force was applied for 5 s. In summary, these pulling experiments demonstrate that apCAM indeed undergoes homophilic binding.

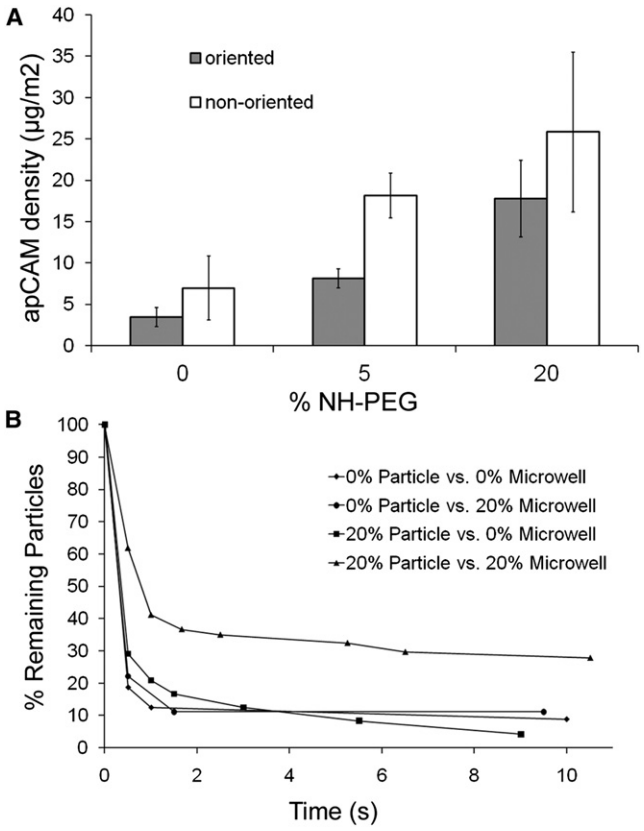

FIGURE 2 (*A*) apCAM surface density as a function of the PEG composition and conjugation chemistry employed. apCAM was detected by an HRP-based colorimetric assay using 4E8 antibody. Oriented conjugation was achieved via the His_6-tag located at the C-terminus of the protein. Nonoriented conjugation was achieved via primary amines. (*B*) Specificity of the particle-pulling experiment. Less than 12.5% of particles formed nonspecific adhesions, as determined by the fraction of bound particles at 5 s during 6.5 pN constant-force pulling.

Bond formation is a function of time and apCAM coverage

Bond formation was determined by observing the restricted planar movement of the particles on microwell surfaces. Data are expressed as the root mean-square displacement (RMSD) divided by the time period between two consecutive images (ΔT). Particle RMDS/ΔT histograms (Fig. 3 *A*) suggested that a threshold of 0.75 μm/s can discriminate bound particles from unbound particles that are exhibiting planar Brownian motion. The fraction of bound particles increased over time for all apCAM surface densities, indicating the formation of initial contacts between apCAM molecules on opposite surfaces (Fig. 3, *inset*). The diffusion coefficient of the bound particles (averaged over 15 s) also decreased with settling time, suggesting a strengthening in the interaction between apCAM-conjugated surfaces (Fig. 3 *B*).

Bond lifetime decreases with increasing external force

Forced unbinding experiments were conducted using PEG-coated, apCAM-conjugated particle and microwell surfaces at low (8.1 $\mu g/m^2$) and high (17.8 $\mu g/m^2$) apCAM densities. Particles were allowed to settle on microwells for 3 or 6 min before force application. Microwell surfaces were monitored during constant vertical forces of 0.5, 3.3, or 6.5 pN. External force application decreased bond lifetime as a function of force and apCAM surface density. A small increase in applied force from 0.5 pN to 3.3 pN significantly accelerated unbinding for surfaces with low apCAM density, whereas the same increase only slightly accelerated the unbinding for surfaces with higher apCAM density (Fig. 4). When lifetime curves of bonds subjected to the same external force are compared, experiments conducted with different apCAM surface densities can be distinguished (Fig. S4). Increasing the settlement period from 3 min to 6 min drastically increased the bond lifetime for 3.3 pN

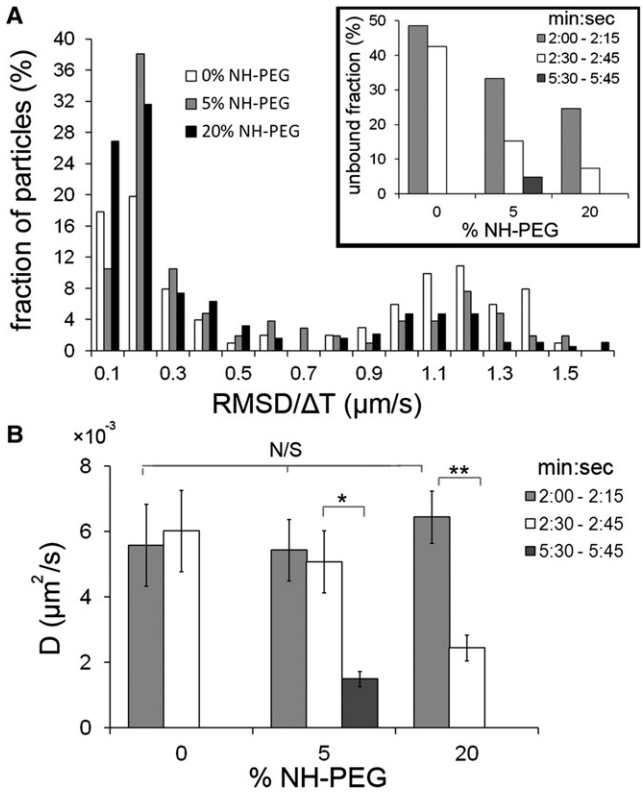

FIGURE 3 (*A*) Particle velocity histogram ($N = 393$ particles) showing the coexistence of bound particles and particles undergoing two-dimensional Brownian movement after 2 min on the microwell surface for different apCAM densities. Inset: The fraction of unbound particles depends on the apCAM surface density and binding time (min/s). (*B*) Change in the diffusion coefficient of bound particles over time (min/s) as a function of apCAM surface density. Bars represent mean ± SE; $N = 564$ particles. N/S: not significant, single-factor analysis of variance ($p > 0.6$); * $p < 0.001$; ** $p < 0.0001$.

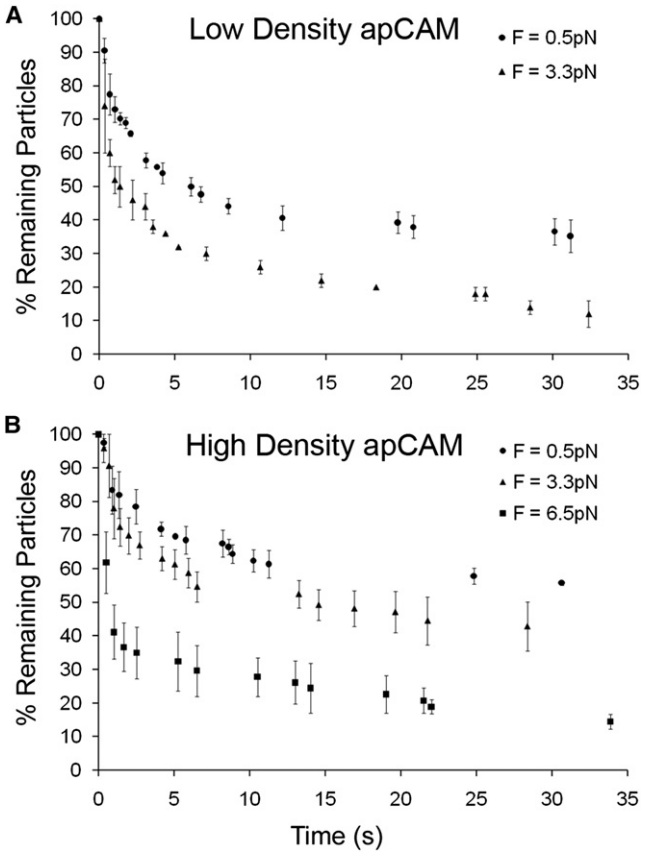

FIGURE 4 Effect of force on bond lifetime at constant apCAM surface density. (*A*) At low densities, a modest increase in force is sufficient to change the bond lifetime drastically. (*B*) At higher densities, higher forces are required to affect the bond lifetime. Bars represent mean ± SE; $N = 3$ independent experiments for each condition with ~50 particles each.

pulling at low apCAM densities (Fig. 5). Particles that were allowed to settle for 6 min and pulled with 6.5 pN had higher bond lifetimes than those that were allowed to settle for 3 min and pulled with 3.3 pN. The force–bond lifetime results are in agreement with the binding results for long-settlement-period experiments. Cumulatively, these results suggest that the forced unbinding of apCAM bonds depends on the duration of bond formation and the availability of apCAM on either surface.

Mathematical modeling predicts two types of bonds

Mathematical models based on biophysical concepts developed for the NCAM-NCAM bond (29,32,35,42) were created and tested for the current experimental results (see Supporting Material). For each model, proposed interdomain interactions (Fig. S1) were characterized by fitting experimental force-bond lifetime curves (curves in Figs. 4 and 5) with k_{on} (on-rate), $k_{off,0}$, f, and n (number of bonds) parameters. The quality of the fit is expressed in total error E, calculated by summing the RMSDs for each bond lifetime curve and the square of the difference between observed and calculated bound fractions before external force application (Fig. 6 *A*). The minimum adjusted coefficient of determination (R^2_{adj}), corresponding to the worst fit, is also shown for each model (see Supporting Material for definition; Fig. 6 *A*). Model L, which predicts two types of bonds ($Ig_{1\text{-}5}$ and $Ig_{\alpha\beta}$; Fig. 6 *B*), provides the best fit. Model parameters and calculated force-bond lifetime curves for high apCAM surface density are shown in Fig. 6, *C* and *D*, respectively (see Fig. S5 for low apCAM density curves). Sensitivity analyses (Fig. S6) and calculated confidence intervals suggest that the scaling forces of Ig_{24} and Ig_{33} cannot be determined accurately. This is because the model predicts that the Ig_{15} interaction will have high affinity and force sensitivity, and therefore will mask the other two Ig domain interactions. To compare the model results directly with literature values, we calculated the effective bond parameters for $Ig_{1\text{-}5}$ bond (see Supporting Material for details) and converted the scaling forces to the distance to the thermodynamic transition barrier $x^* = k_BT/f$ (43). Because the domain interactions are modeled

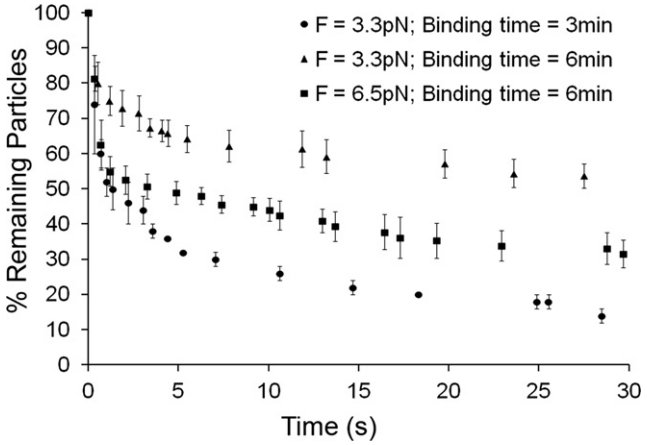

FIGURE 5 Effect of binding period on bond lifetime. The bond lifetime at 3.3 pN pulling increases drastically when the binding time is increased from 3 min to 6 min. When the pulling force is increased to 6.5 pN for this long binding time, a modest decrease in the bond lifetime is observed. Bars represent mean ± SE; $N = 3$ independent experiments for each condition with ~50 particles each.

with first-order kinetics, the k_{on} values are independent of concentration. To express the bond kinetics in terms of dissociation constants (k_D), k_{off}/k_{on} ratios were multiplied with the apparent concentration of apCAM in the contact zone. The k_D values for bonds involving all five or only two Ig domains were determined to be 0.17 and 0.24 μM, respectively. In summary, our modeling results suggest that the homophilic apCAM interaction is mediated by at least two different types of bonds that have similar sensitivities against external force.

DISCUSSION

In this study we applied physiologically relevant constant forces, as exerted by filopodia in growing neurons (44), to apCAM bonds to characterize their kinetic and mechanical properties. Our results show that apCAM undergoes homophilic interactions as predicted based on its vertebrate homolog, NCAM. These findings are consistent with our recent apCAM force spectroscopy data acquired by atomic force microscopy (AFM) (45). External force application decreased the average bond lifetime as predicted by theory (24,25,27,46). Obtained force-bond lifetime curves were fit to a number of theoretical bond models, and the dissociation rate (k_{off}) and characteristic scaling force (f) of each hypothetical Ig domain interaction were determined. Curve-fitting results suggest a bond model with two types of bonds.

The free-energy minima of a biochemical reaction describe various stable states to be reached and energy barriers to be overcome. External mechanical force may affect the energy landscape and thereby change the reaction pathway (see Bustamante et al. (23) for a review). In the case of macromolecular bonds, tilting of the energy landscape may cause an inner activation barrier to emerge as the highest-energy threshold and to dominate the reaction kinetics (46). Because single attachments between two macromolecules often contain multiple interactions, they behave as multiple distinct bonds when subjected to an external force (46). Despite the wide range of bond lifetime curves (Fig. 1 *C*) they exhibit, simplistic single-bond models involving two types of interactions cannot explain the observed apCAM bond behavior. Therefore, we conducted mathematical modeling to explore and compare various conceptual models based on ideas developed for the homolog NCAM. The best fit was provided by model L, which predicts two alternative bond types with similar mechanical properties

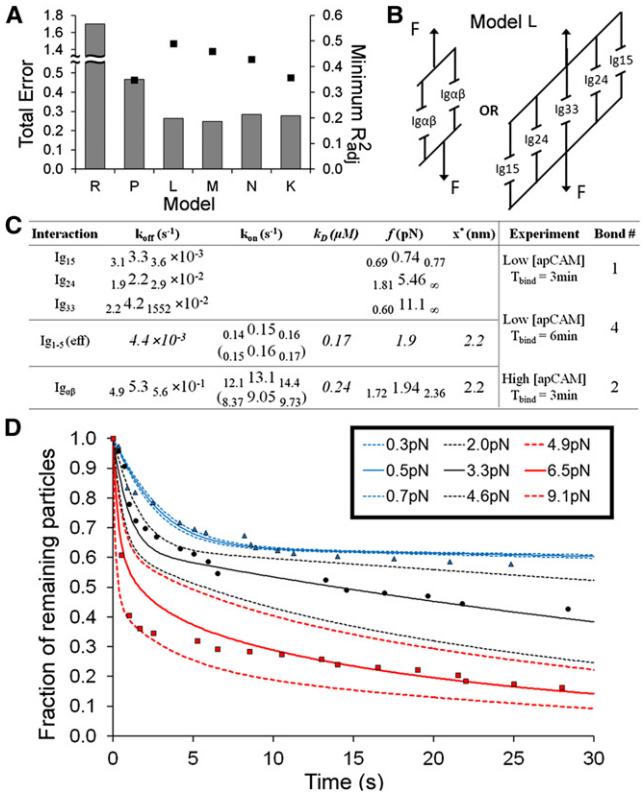

FIGURE 6 Results of the curve-fitting algorithm. (*A*) Comparison of total error E (*bars*) and the minimum of the adjusted coefficient of determination (R^2_{adj}; *dots*), indicating the worst fit of the seven curves for all bond models. R^2_{adj} for model R is negative and therefore is not shown. (*B*) Schematic of model L, which provided the best fit. (*C*) Optimal parameters for model L. Lower and upper bounds of the 95% confidence interval are given in subscript before and after the value, respectively. Calculated values are italicized. Effective k_{off} and f values for $Ig_{1\text{-}5}$ were determined based on model results for individual Ig domain values. Values in parentheses refer to high apCAM surface density. Note that the model is not sensitive to changes in f values for Ig_{24} and Ig_{33} bonds. (*D*) Force–bond lifetime curves for high apCAM surface density data calculated by simulating model L with the parameter set given in *C*. Triangles, circles, and squares represent the experimental data obtained for 0.5, 3.3, and 6.5 pN, respectively. Continuous lines represent model results for 0.5 (*dark gray*; blue in online version; $R^2 = 0.95$), 3.3 (*black*; $R^2 = 0.64$), and 6.5 pN (*light gray*; red in online version; $R^2 = 0.94$) external force. Broken lines represent model results for 0.3, 0.7, 2.0, 4.6, 4.9, and 9.1 pN external force, corresponding to ±40% variation in the applied force.

but different affinities—one involving all five Ig domains in an antiparallel configuration (called $Ig_{1\text{-}5}$), and one involving only two Ig domains. We call the latter bond $Ig_{\alpha\beta}$ because our model cannot distinguish between Ig_{12}, Ig_{23}, etc. interactions. It is remarkable that our curve-fitting algorithm favored a bond model with a relatively low number of free parameters.

The relative roles of individual Ig domains in homophilic NCAM adhesion have been a matter of debate because results obtained by different experimental methods led to contradictory bond models. Binding affinity studies using purified recombinant Ig domains suggested an antiparallel organization in which all Ig domains are involved in binding and the Ig_{33} interaction is the strongest of all (29). However, NMR spectroscopy studies identified binding sites for the Ig_{12} interaction (30,31), leading to an alternative model in which an antiparallel Ig_{12} interaction dominates the NCAM-NCAM adhesion. More recently, based on crystallography and neurite outgrowth assays, a third model was proposed in which Ig_{12} *cis* interactions mediate dimerization of NCAM on each surface, and Ig_{13} or Ig_{23} *trans* interactions mediate the binding of NCAM dimers located on opposite surfaces (34). Force and distance measurements on full-length NCAM ectodomains and domain deletion mutants demonstrated the existence of two distinct interactions, namely, Ig_{12} and Ig_{33}, but not Ig_{13} or Ig_{23} (32), thereby rejecting the third model. AFM single-molecule pulling experiments supported a model in which two mechanically distinct interactions form the NCAM-NCAM bond (33,35) and Ig_{33} and Ig_{12} correspond to the stronger and weaker NCAM bonds, respectively (35). In summary, our results contribute to the notion that IgCAMs share similar binding mechanisms, such as the involvement of multiple types of Ig domain interactions. Although it stems from models developed for NCAM (29,35), our bond model requires differences in both the chemical and mechanical strengths of the individual Ig domain interactions within the $Ig_{1\text{-}5}$ complex.

The majority of studies that have investigated the relationship between force and adhesion bond dynamics used AFM. This technique generates a high number of force-distance curves that are compiled into rupture force histograms, which in turn are used to determine bond characteristics. AFM allows for control of the force rate (typically hundreds to thousands of piconewtons per second) but compromises force resolution. In this study we used a magnetic-tweezers model that enables <0.1 pN resolution and operates in the 0–10 pN range. High force rates are not uncommon in cellular adhesion, such as in the adhesion of immune cells to the vasculature (43); however, low rates (1–10 pN/s) are also observed in adhesion-related cellular events, such as force-induced initiation of neurites (47) or exertion of force by filopodia during axon outgrowth (44). Cell adhesion is a highly dynamic process that requires IgCAM bonds to operate in different force and force rate regimes. In this regard, static force-clamp measurements are complementary to dynamic AFM measurements. The empirical data generated by force-clamp experiments can be directly subjected to Bell's model, and bond properties can be estimated without exhaustive modeling as in the case of AFM (33).

Our experimental results suggest that the apCAM surface density and binding period affect the binding and forced unbinding kinetics. Accordingly, the model predicts an increase in the number of bonds forming between adjacent surfaces when the binding period or the apCAM density is increased. The model also predicts an increase in the fraction of particles bound via $Ig_{1\text{-}5}$ from 47% to 62% with increasing apCAM density. This suggests that the lack of availability of apCAM on surfaces may limit the engagement of the full-length ectodomain and favor the formation of $Ig_{\alpha\beta}$ interactions. One should note that k_{on} represents the binding rate of a diffusing microparticle on a flat surface, rather than the actual on-rate of the molecular interaction that takes place. By calculating an apparent density of apCAM in the contact zone, we estimate the k_{on} values to be 2.6×10^5 and 2.2×10^6 $M^{-1}s^{-1}$ for the two apCAM densities that were used in this study. Using these measured k_{on} and k_{off} values for apCAM, we determined the k_D values for the two bond types to be 0.17 and 0.24 μM, which are weaker than NCAM-NCAM (25 nM (32)) and V-CAM-integrin (11 nM (48)) bonds, but stronger than homophilic VE-cadherin (1 mM–10 μM (49)) and NCAM Ig_{12} (55 μM (50)) bonds. Effective x^* values for both bond types were calculated as 2.2 nm, which are significantly higher than the reported values for other homophilic CAM bonds (N-cadherin: 0.77 nm (51); VE-cadherin: 0.59 nm (52) or 0.42 nm (49); ALCAM: 0.38 nm (53); NCAM: 0.32 nm and 0.17 nm (35); and E-cadherin: 0.32 nm and 0.1 nm (51)).

We recently characterized the apCAM-apCAM interaction using AFM in our laboratory (45). The AFM study also detected strong and weak homophilic apCAM bonds with k_{on} ~2×10^4 $M^{-1}s^{-1}$, $x^* = 0.46 \pm 0.88$ and 0.1 ± 0.06 nm, respectively, and $k_{off} = 0.05 \pm 0.88$ and 0.72 ± 1 s^{-1}, respectively. A comparison of the results obtained from the two techniques needs to be considered in the light of several experimental details. First, the Bell-Evans model was used to analyze the kinetics of the homophilic apCAM interactions for the AFM measurements, which meant that the apparent increase in adhesion force was determined as a function of increasing rate of applied force. The application of the Bell-Evans model clearly introduced a high level of uncertainty to the measurement of k_{off}, and the error was so high for the strong bond that the k_{off} value was considered to be unreliable. There was also a high level of uncertainty in the value of k_{on} due to the uncertainty in the calculation of the effective concentration of apCAM on the tip of the AFM probe. Second, apCAM had to be covalently immobilized in the AFM study because it was found that the His_6-NTA

bond failed after several hundred single force measurements. The magnetic-tweezers technique uses a large number of probes to measure single rupture events; therefore, His_6-NTA chemistry could be used to conjugate the apCAM molecules for these measurements. We speculate that the random orientation of apCAM molecules resulting from the covalent chemistry may reduce the apparent force sensitivity, which would explain the lower scaling forces observed in the magnetic-tweezers measurements. However, the magnetic-tweezers unbinding reaction also took place over a much longer time period, and thus the low scaling forces could be indicative of a different free-energy reaction landscape (54). From a biological point of view, high affinity and high sensitivity may be desirable for apCAMs, which are primarily used for neuronal synapse formation and maturation. Such bonds would facilitate long-term connections but permit the bond to break under low retraction forces once the synapse is no longer needed.

In an attempt to explore the interaction between apCAM-conjugated microspheres and *Aplysia* bag cell neuron growth cones, we added particles to cultured neurons (not shown). Microspheres that fell onto the peripheral zone of the growth cone rapidly moved to the transition zone through actin flow coupling and remained attached to the cell surface when subjected to 10 pN vertical force for >5 min. Consistent with the holographic optical tweezers results (21) and apCAM beads physically restrained with a micropipette (20), these observations indicate a strong coupling between the membrane apCAM and the underlying actin cytoskeleton. This suggests that, as opposed to a rigid, flat surface with a monolayer of PEG, the plasma membrane is able to deform to engulf microparticles. This allows numerous apCAM bonds to form due to increased contact area. The formation and breakage of apCAM bonds on live neurons are beyond the scope of this work; however, these observations indicate that cell-based force-clamp experiments require experimental setups that can deliver forces on the order of 100 pNs.

This study confirms the homophilic binding properties of apCAM and demonstrates that magnetic tweezers are suitable for characterizing relatively weak molecular interactions between IgCAM molecules subjected to constant forces. Regardless of the experimental method employed, single-molecule force clamps are powerful tools for measuring bond kinetics (55). Recent advances in magnetic (56) and optical (57) sensing modalities, as well as novel microfabrication techniques (58), are paving the way for massively parallel, multiplexed magnetic-tweezers experiments. These systems will not only facilitate biophysical characterization of molecular interactions but also enable high-content screening for medical applications.

CONCLUSIONS

To our knowledge, this study represents the first application of piconewton-level constant forces via magnetic tweezers on IgCAM bonds. We have shown that apCAM undergoes homophilic binding involving relatively low adhesion forces. An analysis of the force-bond lifetime relation suggests that Ig domain interactions within the apCAM bond complex have affinity constants and characteristic scaling forces in the range of values that have been reported for other CAM bonds and obtained by other methods. Mathematical modeling suggests that only those bond models that incorporate multiple bond types can fit the forced unbinding curves. This level of complexity may be beneficial for CAMs that are to operate in different force and force rate regimes.

SUPPORTING MATERIAL

Additional details and references (59–61) are available at http://www.biophysj.org/biophysj/supplemental/S0006-3495(12)00915-0.

We thank Dr. Mark Platt for his suggestions regarding surface chemistry, Dr. Elena Martines and Mr. Fernando Mancilla Perez for the *Aplysia* neurons, and Dr. Ying Xiong for her initial work on bond theory. We also thank Kelsey Martin, Samuel Schacher, and Eric Kandel for providing the original apCAM construct, which was used to make a baculovirus construct of the extracellular apCAM region, as well as for 4E8 hybridoma cells.

This material is based on works supported by the Science Foundation Ireland under grants 08/RP1/B1376 and 08/IN1/B2072 (to G.U.L.) and the National Institutes of Health (R01 NS049233 to D.M.S.). A.B. received support from the Erasmus Student Mobility for Placements Programme of the European Commission.

REFERENCES

1. Vogel, V., and M. Sheetz. 2006. Local force and geometry sensing regulate cell functions. *Nat. Rev. Mol. Cell Biol.* 7:265–275.
2. Johnson, C. P., H. Y. Tang, …, D. E. Discher. 2007. Forced unfolding of proteins within cells. *Science.* 317:663–666.
3. Hoffman, B. D., C. Grashoff, and M. A. Schwartz. 2011. Dynamic molecular processes mediate cellular mechanotransduction. *Nature.* 475:316–323.
4. Vogel, V. 2006. Mechanotransduction involving multimodular proteins: converting force into biochemical signals. *Annu. Rev. Biophys. Biomol. Struct.* 35:459–488.
5. Aricescu, A. R., and E. Y. Jones. 2007. Immunoglobulin superfamily cell adhesion molecules: zippers and signals. *Curr. Opin. Cell Biol.* 19:543–550.
6. Cavallaro, U., and E. Dejana. 2011. Adhesion molecule signalling: not always a sticky business. *Nat. Rev. Mol. Cell Biol.* 12:189–197.
7. Maness, P. F., and M. Schachner. 2007. Neural recognition molecules of the immunoglobulin superfamily: signaling transducers of axon guidance and neuronal migration. *Nat. Neurosci.* 10:19–26.
8. Burnette, D. T., A. W. Schaefer, …, P. Forscher. 2007. Filopodial actin bundles are not necessary for microtubule advance into the peripheral domain of Aplysia neuronal growth cones. *Nat. Cell Biol.* 9:1360–1369.
9. Medeiros, N. A., D. T. Burnette, and P. Forscher. 2006. Myosin II functions in actin-bundle turnover in neuronal growth cones. *Nat. Cell Biol.* 8:215–226.
10. Zhang, X. F., A. W. Schaefer, …, P. Forscher. 2003. Rho-dependent contractile responses in the neuronal growth cone are independent of classical peripheral retrograde actin flow. *Neuron.* 40:931–944.

11. Grzywa, E. L., A. C. Lee, …, D. M. Suter. 2006. High-resolution analysis of neuronal growth cone morphology by comparative atomic force and optical microscopy. *J. Neurobiol.* 66:1529–1543.

12. Xiong, Y., A. C. Lee, …, G. U. Lee. 2009. Topography and nanomechanics of live neuronal growth cones analyzed by atomic force microscopy. *Biophys. J.* 96:5060–5072.

13. Schaefer, A. W., V. T. Schoonderwoert, …, P. Forscher. 2008. Coordination of actin filament and microtubule dynamics during neurite outgrowth. *Dev. Cell.* 15:146–162.

14. Lee, A. C., and D. M. Suter. 2008. Quantitative analysis of microtubule dynamics during adhesion-mediated growth cone guidance. *Dev. Neurobiol.* 68:1363–1377.

15. Mayford, M., A. Barzilai, …, E. R. Kandel. 1992. Modulation of an NCAM-related adhesion molecule with long-term synaptic plasticity in Aplysia. *Science.* 256:638–644.

16. Keller, F., and S. Schacher. 1990. Neuron-specific membrane glycoproteins promoting neurite fasciculation in Aplysia californica. *J. Cell Biol.* 111:2637–2650.

17. Bailey, C. H., M. Chen, …, E. R. Kandel. 1992. Serotonin-mediated endocytosis of apCAM: an early step of learning-related synaptic growth in Aplysia. *Science.* 256:645–649.

18. Lee, S.-H., C.-S. Lim, …, B. K. Kaang. 2007. Nuclear translocation of CAM-associated protein activates transcription for long-term facilitation in Aplysia. *Cell.* 129:801–812.

19. Thompson, C., C. H. Lin, and P. Forscher. 1996. An Aplysia cell adhesion molecule associated with site-directed actin filament assembly in neuronal growth cones. *J. Cell Sci.* 109:2843–2854.

20. Suter, D. M., L. D. Errante, …, P. Forscher. 1998. The Ig superfamily cell adhesion molecule, apCAM, mediates growth cone steering by substrate-cytoskeletal coupling. *J. Cell Biol.* 141:227–240.

21. Mejean, C. O., A. W. Schaefer, …, E. R. Dufresne. 2009. Multiplexed force measurements on live cells with holographic optical tweezers. *Opt. Express.* 17:6209–6217.

22. Suter, D. M., and P. Forscher. 2001. Transmission of growth cone traction force through apCAM-cytoskeletal linkages is regulated by Src family tyrosine kinase activity. *J. Cell Biol.* 155:427–438.

23. Bustamante, C., Y. R. Chemla, …, D. Izhaky. 2004. Mechanical processes in biochemistry. *Annu. Rev. Biochem.* 73:705–748.

24. Bell, G. I. 1978. Models for the specific adhesion of cells to cells. *Science.* 200:618–627.

25. Evans, E., and K. Ritchie. 1997. Dynamic strength of molecular adhesion bonds. *Biophys. J.* 72:1541–1555.

26. Williams, P. M. 2003. Analytical descriptions of dynamic force spectroscopy: behaviour of multiple connections. *Anal. Chim. Acta.* 479:107–115.

27. Evans, E. A., and D. A. Calderwood. 2007. Forces and bond dynamics in cell adhesion. *Science.* 316:1148–1153.

28. Shang, H., and G. U. Lee. 2007. Magnetic tweezers measurement of the bond lifetime-force behavior of the IgG-protein A specific molecular interaction. *J. Am. Chem. Soc.* 129:6640–6646.

29. Ranheim, T. S., G. M. Edelman, and B. A. Cunningham. 1996. Homophilic adhesion mediated by the neural cell adhesion molecule involves multiple immunoglobulin domains. *Proc. Natl. Acad. Sci. USA.* 93:4071–4075.

30. Jensen, P. H., V. Soroka, …, F. M. Poulsen. 1999. Structure and interactions of NCAM modules 1 and 2, basic elements in neural cell adhesion. *Nat. Struct. Biol.* 6:486–493.

31. Atkins, A. R., M. J. Osborne, …, H. J. Dyson. 1999. Association between the first two immunoglobulin-like domains of the neural cell adhesion molecule N-CAM. *FEBS Lett.* 451:162–168.

32. Johnson, C. P., I. Fujimoto, …, D. Leckband. 2004. Mechanism of homophilic adhesion by the neural cell adhesion molecule: use of multiple domains and flexibility. *Proc. Natl. Acad. Sci. USA.* 101: 6963–6968.

33. Hukkanen, E. J., J. A. Wieland, …, R. D. Braatz. 2005. Multiple-bond kinetics from single-molecule pulling experiments: evidence for multiple NCAM bonds. *Biophys. J.* 89:3434–3445.

34. Soroka, V., K. Kolkova, …, C. Kasper. 2003. Structure and interactions of NCAM Ig1-2-3 suggest a novel zipper mechanism for homophilic adhesion. *Structure.* 11:1291–1301.

35. Wieland, J. A., A. A. Gewirth, and D. E. Leckband. 2005. Single molecule adhesion measurements reveal two homophilic neural cell adhesion molecule bonds with mechanically distinct properties. *J. Biol. Chem.* 280:41037–41046.

36. Shang, H., W. S. Chang, …, G. U. Lee. 2006. Synthesis and characterization of paramagnetic microparticles through emulsion-templated free radical polymerization. *Langmuir.* 22:2516–2522.

37. Reference deleted in proof.

38. Sagvolden, G., I. Giaever, and J. Feder. 1998. Characteristic protein adhesion forces on glass and polystyrene substrates by atomic force microscopy. *Langmuir.* 14:5984–5987.

39. Suter, D. M., A. W. Schaefer, and P. Forscher. 2004. Microtubule dynamics are necessary for SRC family kinase-dependent growth cone steering. *Curr. Biol.* 14:1194–1199.

40. Rao, S. 2009. Engineering Optimization: Theory and Practice. John Wiley & Sons, Hoboken, NJ.

41. Zhu, X. Y., Y. Jun, …, A. Guo. 2001. Grafting of high-density poly(ethylene glycol) monolayers on Si(111). *Langmuir.* 17:7798–7803.

42. Maruthamuthu, V., K. Schulten, and D. Leckband. 2009. Elasticity and rupture of a multi-domain neural cell adhesion molecule complex. *Biophys. J.* 96:3005–3014.

43. Evans, E., A. Leung, …, S. Simon. 2001. Chemically distinct transition states govern rapid dissociation of single L-selectin bonds under force. *Proc. Natl. Acad. Sci. USA.* 98:3784–3789.

44. Cojoc, D., F. Difato, …, V. Torre. 2007. Properties of the force exerted by filopodia and lamellipodia and the involvement of cytoskeletal components. *PLoS ONE.* 2:e1072.

45. Martines, E., J. Zhong, …, G. U. Lee. 2012. Single molecule force spectroscopy of the *Aplysia* cell adhesion molecule reveals two homophilic bonds. *Biophys. J.* http://dx.doi.org/10.1016/j.bpj.2012.07.004.

46. Evans, E. 2001. Probing the relation between force—lifetime—and chemistry in single molecular bonds. *Annu. Rev. Biophys. Biomol. Struct.* 30:105–128.

47. Fass, J. N., and D. J. Odde. 2003. Tensile force-dependent neurite elicitation via anti-β1 integrin antibody-coated magnetic beads. *Biophys. J.* 85:623–636.

48. Woodside, D. G., R. M. Kram, …, P. Vanderslice. 2006. Contrasting roles for domain 4 of VCAM-1 in the regulation of cell adhesion and soluble VCAM-1 binding to integrin $\alpha 4\beta 1$. *J. Immunol.* 176:5041–5049.

49. Baumgartner, W., P. Hinterdorfer, …, D. Drenckhahn. 2000. Cadherin interaction probed by atomic force microscopy. *Proc. Natl. Acad. Sci. USA.* 97:4005–4010.

50. Kiselyov, V. V., V. Berezin, …, E. Bock. 1997. The first immunoglobulin-like neural cell adhesion molecule (NCAM) domain is involved in double-reciprocal interaction with the second immunoglobulin-like NCAM domain and in heparin binding. *J. Biol. Chem.* 272:10125–10134.

51. Panorchan, P., M. S. Thompson, …, D. Wirtz. 2006. Single-molecule analysis of cadherin-mediated cell-cell adhesion. *J. Cell Sci.* 119:66–74.

52. Panorchan, P., J. P. George, and D. Wirtz. 2006. Probing intercellular interactions between vascular endothelial cadherin pairs at single-molecule resolution and in living cells. *J. Mol. Biol.* 358:665–674.

53. Te Riet, J., A. W. Zimmerman, …, F. de Lange. 2007. Distinct kinetic and mechanical properties govern ALCAM-mediated interactions as shown by single-molecule force spectroscopy. *J. Cell Sci.* 120:3965–3976.

54. Suzuki, Y., and O. K. Dudko. 2011. Biomolecules under mechanical stress: a simple mechanism of complex behavior. *J. Chem. Phys.* 134:065102.

55. Liang, J., and J. M. Fernández. 2011. Kinetic measurements on single-molecule disulfide bond cleavage. *J. Am. Chem. Soc.* 133:3528–3534.

56. Gaster, R. S., L. Xu, …, S. X. Wang. 2011. Quantification of protein interactions and solution transport using high-density GMR sensor arrays. *Nat. Nanotechnol.* 6:314–320.

57. Bruls, D. M., T. H. Evers, …, M. W. Prins. 2009. Rapid integrated biosensor for multiplexed immunoassays based on actuated magnetic nanoparticles. *Lab Chip.* 9:3504–3510.

58. De Vlaminck, I., T. Henighan, …, C. Dekker. 2011. Highly parallel magnetic tweezers by targeted DNA tethering. *Nano Lett.* 11:5489–5493.

59. Tanase, M., N. Biais, and M. Sheetz. 2007. Magnetic tweezers in cell biology. *Methods Cell Biol.* 83:473–493.

60. Sbalzarini, I. F., and P. Koumoutsakos. 2005. Feature point tracking and trajectory analysis for video imaging in cell biology. *J. Struct. Biol.* 151:182–195.

61. Motulsky, H. J., and A. Christopoulos. 2003. Fitting Models to Biological Data Using Linear and Nonlinear Regression: A Practical Guide to Curve Fitting. GraphPad Software Inc., San Diego.